energies

Article

Technical Analysis of the Possibility of Burning Hydrogen in Furnaces of the Metallurgical Sector

Andrzej Gołdasz, Karol Sztekler * and Łukasz Mika

Department of Thermal and Fluid Flow Machines, Faculty of Energy and Fuels, AGH University of Krakow, al. A. Mickiewicza 30, 30-059 Krakow, Poland; goldasz@agh.edu.pl (A.G.); lmika@agh.edu.pl (Ł.M.)
* Correspondence: sztekler@agh.edu.pl

Abstract: This article analyses the possibility of using hydrogen as fuel in furnaces used in the metallurgical industry. The research was conducted for a selected continuous furnace. For this purpose, based on actual measurements, a heat balance of the furnace was prepared to determine its energy indicators. These values were used to verify the developed numerical model in IPSEpro 7.0 software. Numerical calculations were performed for three variants: pure natural gas; 30% hydrogen, 70% natural gas; and 100% hydrogen. The determined values of gas and combustion air streams allowed for achieving the assumed charge temperature in the heating technology. Calculations of the impact of the excess combustion air ratio on process parameters were also carried out. It was found that no changes are required in the exhaust gas removal system, but verification of the fan supplying air to cool the exhaust gases before the recuperator is necessary. The amount of hydrogen required to fuel the continuous furnace also increases significantly (nearly threefold), which may also affect operating costs. At the same time, the emission of carbon dioxide into the atmosphere is completely reduced, which may be an important criterion when considering modernization options for heating furnaces in the metallurgical industry.

Keywords: hydrogen; combustion; renewable energy sources walking-beam furnace

Citation: Gołdasz, A.; Sztekler, K.; Mika, Ł. Technical Analysis of the Possibility of Burning Hydrogen in Furnaces of the Metallurgical Sector. *Energies* **2024**, *17*, 4733. https://doi.org/10.3390/en17184733

Academic Editor: Mariola Saternus

Received: 21 August 2024
Revised: 17 September 2024
Accepted: 20 September 2024
Published: 23 September 2024

1. Introduction

1.1. Electricity Consumption

According to a regulation published in October 2022, European Union countries declared the implementation of emergency measures to reduce energy prices and assist both businesses and households. An essential measure is to reduce the consumption of electricity by at least 5% during peak hours [1].

The industry is the area characterised by the highest electricity consumption (Figure 1). In 2020, the electricity used by the industrial sector in the EU was 855 TWh. However, the increase in electricity consumption over recent years was mainly accounted for by the rapidly growing sectors of services and households. Between 2000 and 2020, electricity consumption in the service sector increased by as much as 24.3%. Regarding households, they increased their electricity use by 17.7% over the same period and, for the first time in 2006, had higher electricity consumption than the service industry. The transport sector, on the other hand, is characterised by a constant level of electricity consumption over the years [2].

The characteristic curves of electricity consumption in Poland by sector are similar to the level in the other EU countries (Figure 2). The largest increase in electricity consumption is again associated with the broadly defined service sector. Between 2000 and 2020, electricity use in this sector increased by as much as 73%. There is also a significant increase in electricity demand in households (43%) and in the rapidly growing industrial sector (36%) [2].

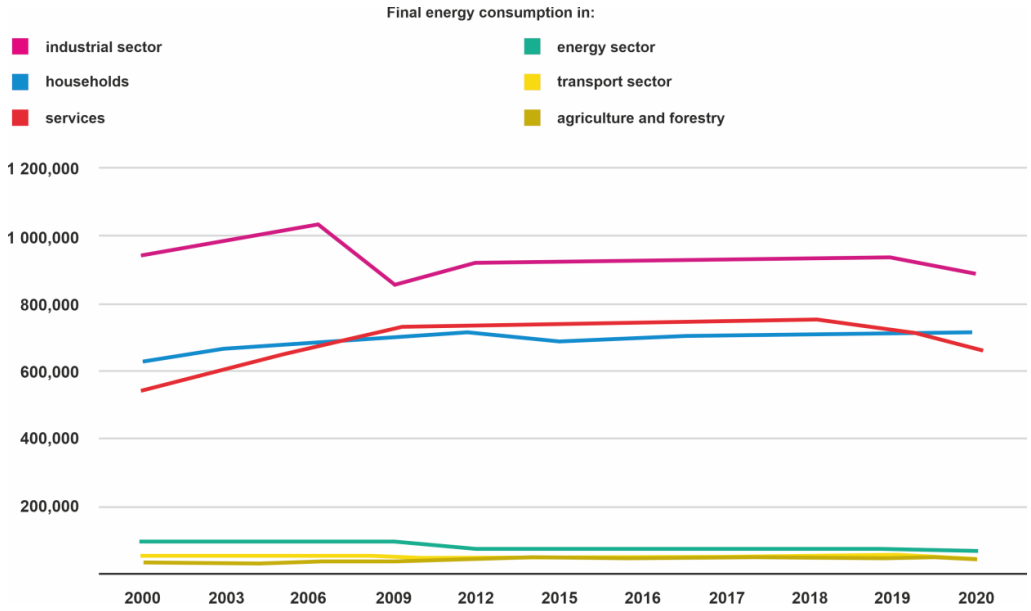

Figure 1. Gross electricity consumption GWh, EU, 2000–2020 [2].

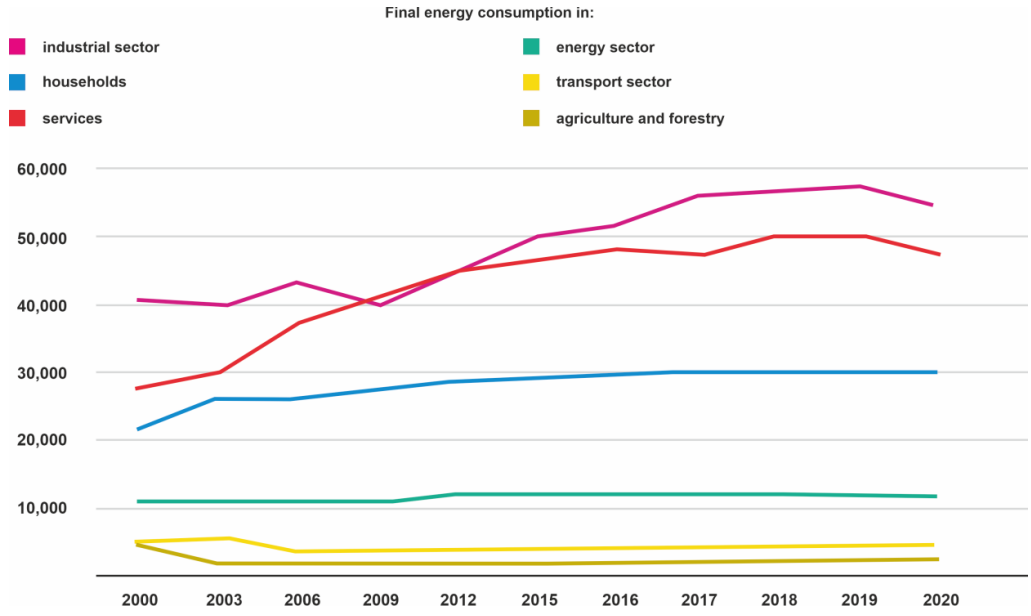

Figure 2. Gross electricity consumption GWh, PL, 2000–2020 [2].

The volume of electricity consumption in households depends on the types of electrical devices used by the residents according to their standard of living. The total value of electricity demand in the residential group is influenced by both the quantity and quality of dwellings and appliances, as well as their mode of operation. The per capita consumption of electricity in the area of households among EU member states in 2020 was 1.6 MWh (Table 1). The per capita electricity use in the aforementioned sector varied significantly. Values ranged from less than 1 MWh in Poland and some other countries to 4 MWh in Sweden and Finland [2].

Table 1. Per capita consumption of electricity in the sector of households, EU, 2020 [2].

Country	Per Capita Consumption (MWh)
EU	0.8
Romania	0.9
Poland	1
Latvia	1.2
Slovakia	1.3
Italy	1.5
Lithuania	1.6
Hungary	1.7
Portugal	1.8
Netherlands	1.9
Czechia	2
Croatia	2.1
Luxembourg	2.2
Estonia	2.3
Belgium	2.4
Greece	2.5
Bulgaria	2.6
Malta	2.7
Slovenia	2.8
Ireland	2.9
Germany	3
Spain	3.1
Denmark	3.2
Austria	3.3
Cyprus	3.5
France	3.7
Finland	3.9
Sweden	4.3

1.2. Use of Hydrogen in Industry

The adoption of the EU Hydrogen Strategy by the member states in July 2022 was the reason why hydrogen came to the forefront of the European energy transition debate. Its multifunctionality and wide range of applications have given it the potential to be one of the key factors in the decarbonisation of the economy. The properties that make H_2 an interesting energy carrier include its higher volumetric energy density than batteries, its ability to be stored for long periods of time, and its suitability for the production of other gases. In addition, its use for energy purposes does not produce greenhouse gas emissions, and existing building facilities for gas transport and storage can be adapted for hydrogen transmission and storage in a relatively short time [3]. The role of hydrogen in the energy mix is shown in Figure 3.

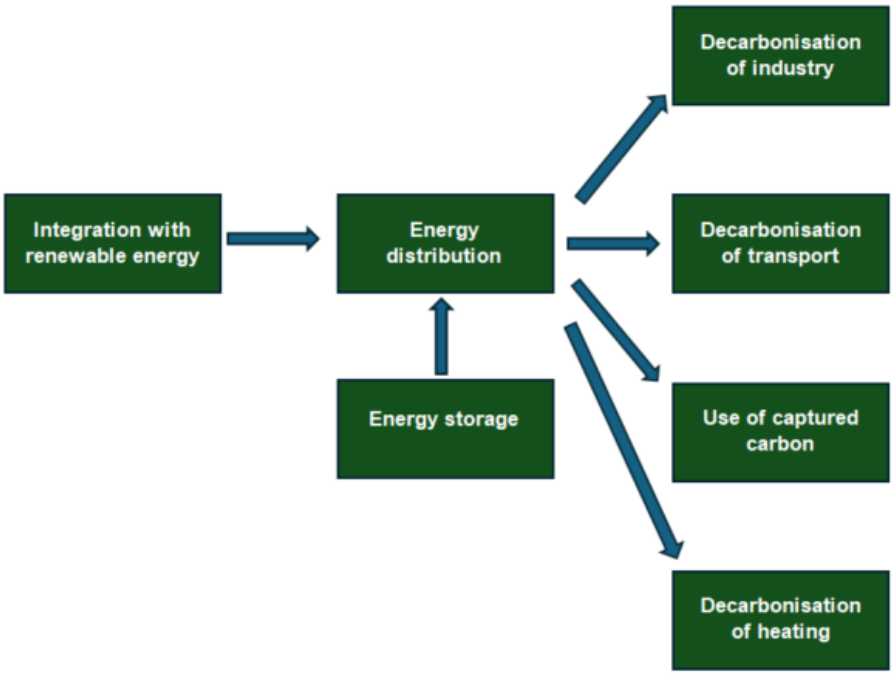

Figure 3. The structure of hydrogen energy industry.

Due to the above-mentioned properties, hydrogen has found use in the stationary energy sector. Among other things, it is used in the production of electricity.

The concept of creating sources of emergency power supply is highly valued nowadays. For this reason, it is becoming increasingly common to hear about the possibility of supplying energy to off-grid systems using fuel cells that can use methanol or natural gas as fuel in addition to hydrogen. The role of alternative generators is important for the operation of the energy sector as they ensure the continuous operation and protection of the equipment connected to the system. This is particularly relevant to the IT and telecommunications sectors.

Fuel cells compare much more favourably against conventional CHP plants in terms of electrical efficiency, even in the case of small systems. As a result, they produce a significant amount of electricity with little heat production. The advantages of using fuel cells as emergency power sources include extended autonomous operation and long lifespan, low operating costs, as well as emission-free and quiet electricity generation. The backup power of the described cells ranges from a few kW to more than 1 GWe. Many types of fuel cells are used in stationary systems. It is also possible to use them for cooling [4]. The products of the CHP (combined heat and power) used in domestic systems based on combined generation, are referred to as micro-CHP. This type of system can work in two ways—either the system covers most of the electricity demand or the heat demand. If electricity prices in the market are high, the optimal mode of operation is the one focused on power generation. This makes it possible to minimise the energy supplied from outside or to feed excess energy back into the grid. The heat, which is a by-product of the CHP plant, is used to cover part of the heat demand for the building. The missing part is supplemented by an auxiliary heating system. Fuel cells are therefore best suited to homes with low heat demand. The most common power rating for CHP systems is between 0.7 and 5 kWe. Systems of this type use PEM and SO fuel cells. The process that makes fuel cells attractive is the direct electrochemical conversion during heat and power generation and the associated higher electrical efficiency. In combined-mode operation, fuel cells can achieve efficiencies of up to 95%. Electrical efficiency, on the other hand, is roughly 45% [4].

In the metallurgical industry, the prospects for the use of hydrogen are currently related to steel production, where it is used in the process of reducing iron ore instead of coke, thus significantly reducing CO_2 emissions. This is the technology that will be used by,

among others, the steelworks currently under construction in Sweden (as part of the Hybrit project). It is estimated that launching steel production using hydrogen in Sweden alone will reduce CO_2 emissions by 10% [5]. A similar technology is being developed as part of the Green Steel project in Krakow. The International Energy Agency (IEA) has presented a roadmap for the metallurgical industry (Table 2). According to various strategies, hydrogen might account for an 8% reduction in CO_2 emissions by 2050 [6].

Table 2. Reduction of CO_2 emissions by 2050 in the metallurgical industry [6].

Cumulative Direct Emission Reductions between 2020 and 2050	
Technology/Mitigation Strategy	**Contribution (%)**
Material Efficiency	40%
Technology Performance	21%
Carbon Capture, Utilisation, and Storage (CCUS)	16%
Electrification	4%
Hydrogen	8%
Bioenergy	6%
Other Fuel Shifts	5%

These figures can be increased by using hydrogen as a fuel to power the furnaces used in steel forming and heat treatment. Unfortunately, in this case, there is a lack of suitable burners to carry out the process of combustion, characterised by the lack of temperature increase in the furnace chamber and NO_x emissions at an acceptable level.

1.3. Methods of Hydrogen Production

Hydrogen production processes using different technologies are shown schematically in Figure 4.

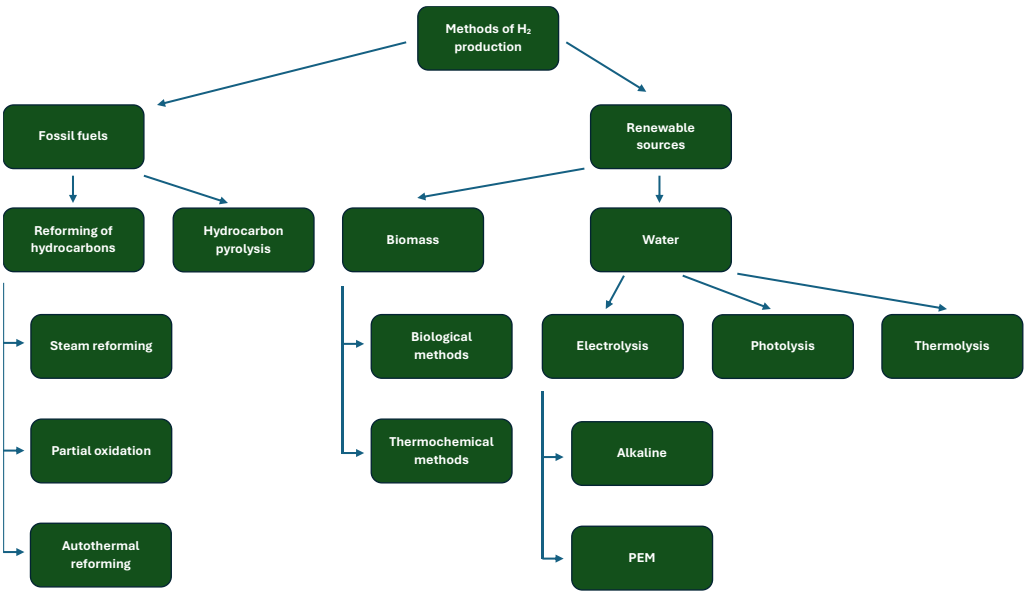

Figure 4. Methods of hydrogen production.

1.4. The Market for Hydrogen Production in Europe and Poland

The European Union has seen intensive development of hydrogen production over the last few years. By the end of 2020, 504 operational hydrogen production sites were identified in European countries. Their total production capacity is 11.5 m tonnes per year. The leading producers include Germany, the Netherlands, Poland, Italy, France, Spain, the

UK and Belgium, which altogether account for 74% of the total hydrogen production in the EU (Table 3). The remaining 18 countries (Table 3) contribute a trace amount to Europe's hydrogen sector. The significant divergences are due to the different levels of industrial development in the individual countries [7]. Poland, in third place, mainly produces the grey type, which is then used by the chemical, refining and food industries. The national leader in the industry is Grupa Azoty, responsible for 32.3% of hydrogen production [8].

Table 3. Total hydrogen production capacity by country, 2020, EU [7].

Country	Million Tonnes per Year
Germany	2.09
Netherlands	1.55
Poland	1.03
Italy	0.85
France	0.82
Spain	0.79
United Kingdom	0.78
Belgium	0.57
Greece	0.39
Norway	0.29
Lithuania	0.27
Hungary	0.26
Romania	0.24
Sweden	0.24
Bulgaria	0.22
Slovakia	0.21
Finland	0.19
Austria	0.17
Portugal	0.16
Croatia	0.15
Czechia	0.13
Denmark	0.03
Switzerland	0.02
Ireland	0.01
Slovenia	0
Iceland	0

In order to accurately depict the structure of hydrogen production in Europe, a distinction is made according to the different production processes. This allows us to distinguish between hydrogen utilised by companies for their own purposes and hydrogen for the commercial market. The first group includes hydrogen produced by steam reforming, partial oxidation, gasification and autothermal reforming of fossil fuels, which is then used by the producer. Also included in this set is hydrogen produced as a by-product of other industrial processes and subsequently used by the refinery for its own purposes. The second variant, in contrast to the first, concerns hydrogen intended for sale. Another group, accounting for only 0.5% of the total production, concerns reforming combined with the capture of carbon dioxide emissions. Hydrogen is also distinguished as a by-product obtained during

electrolysis (3.7%) or from ethylene or styrene. The last of the power-to-hydrogen categories refers to the production of hydrogen in the process of splitting water during electrolysis [7].

Among the top eight hydrogen producers in Europe, hydrogen is predominantly produced in order to meet the needs of the energy sector of the state. Only an insignificant number of companies are involved in trading hydrogen. The amount of hydrogen produced as a by-product also attracts attention. Electrolysis, the most environmentally friendly process, still only accounts for a small percentage of production.

1.5. Combustion of Hydrogen

The very low density of hydrogen, compared with methane, makes the calorific value of hydrogen per unit mass almost 2.4 times greater than that of methane, which in turn makes hydrogen an attractive fuel. At the same time, the very low density of hydrogen affects the geometry of the system for supplying fuel to the heating appliance. As a result, three times as much fuel must be pumped in the same amount of time to deliver the same amount of energy. An important parameter affecting the stability of the flame is the flame speed, which, in the case of hydrogen, is 1.7 m/s and is more than 4.4 times greater than that of methane. Failure to adapt the combustion chamber to the increased flame speed can lead to flashback. Another problem in designing equipment intended for hydrogen combustion is the high combustion temperature, which is 2380 K (methane has 2236 K). A direct effect of the high temperature is the increased amount of nitrogen oxides formed through the Zeldovich mechanism [9]. The above aspects cause specific problems in the design of burners intended for use in metallurgical furnaces.

With these aspects of hydrogen combustion in mind, the development of burner design is heading towards the co-firing of hydrogen and natural gas. Usually, the addition of natural gas does not exceed 30%. This amount of natural gas significantly reduces the combustion temperature of the mixture and lowers its rate of combustion (Figure 5).

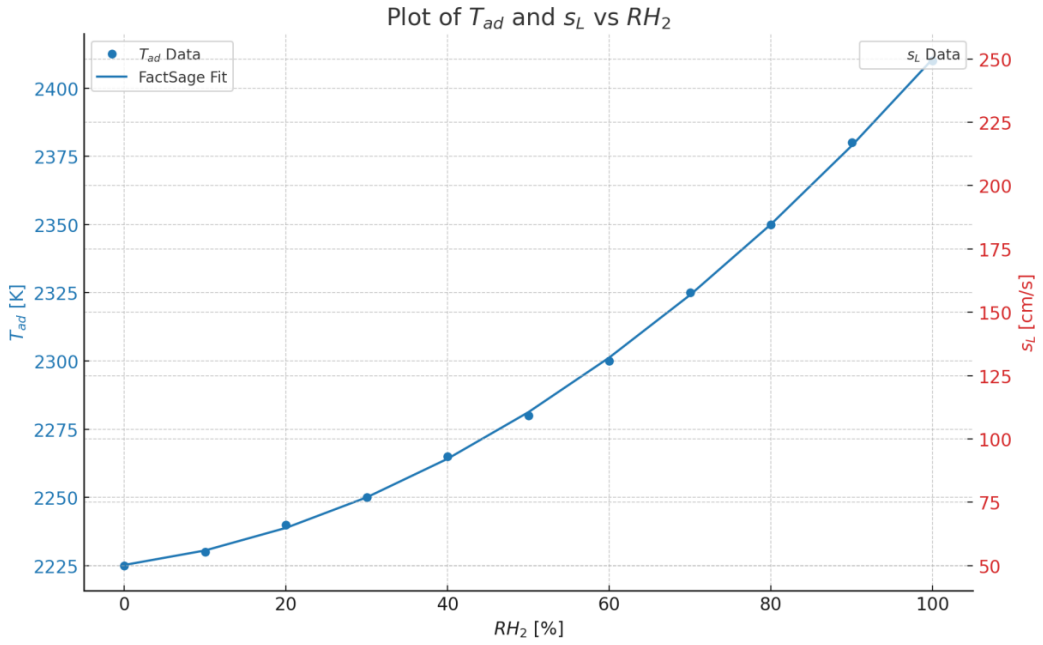

Figure 5. Influence of the proportion of hydrogen in a CH_4/H_2 mixture on laminar flame speed and combustion temperature.

Apart from the appropriate temperature, the heating of the charge in metallurgical furnaces uses the thermal radiation from gaseous products of combustion, which consist largely of CO_2 and H_2O. As a result, a uniform temperature distribution throughout the entire volume of the combustion chamber is achieved. The combustion of hydrogen will remove carbon dioxide from the exhaust gas, which may consequently disturb the

temperature distribution in the chamber [10]. Given the problems with increased NO_x emissions and the lack of conclusive test results on the effect of changing the exhaust gas atmosphere on the temperature distribution in the furnace chamber, it should be considered that the maximum proportion of hydrogen in the mixture with natural gas should not exceed 70%. The Honeywell Company is in possession of designs of such burners.

Burners using 100% hydrogen in the combustion process have been developed by Toyota. However, apart from press releases, there is no clear information on the possibility of utilising them in the metallurgical industry.

2. Description and Heat Balance of the Research Object

The analysis was performed for a walking-beam furnace with working chamber dimensions of 18,600 mm in length, and 15,600 mm in width (Figure 1). A steel charge with a cross-section of 160 × 160 mm and a length of 15,000 mm is heated in the furnace. Natural gas is used as fuel. In order to determine the condition of the furnace prior to retrofitting, a heat balance was carried out during the heating of 69 pieces comprising the B500SP steel charge to a temperature of 1175 °C. The measurements of the temperature of the charge and the atmosphere of the furnace were made using the Datapaq Slab Reheat System (Figure 1). Type K thermocouples in a 3 mm diameter Nicrobell sheath were used to measure the temperature [11]. Figure 6 shows the temperature distribution for points axially aligned with the charge (a) and with exhaust gas (b) during the process.

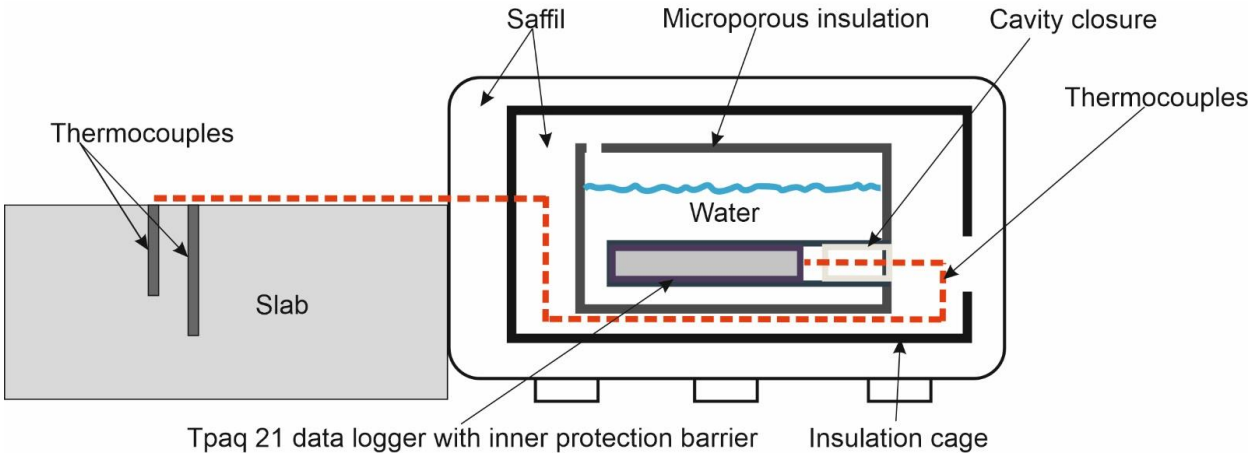

Figure 6. Cross-section of the Datapaq Slab Reheat System.

When analysing the temperature fluctuations at selected points along the charge axis (Figure 7a), it is clear that there is a large asymmetry in the temperature distribution across the width of the walking-beam furnace under consideration. The temperature difference during heating between points 1 and 3 reaches up to 120 °C. It is only at the exit from the alignment zone that this difference drops to about 20 °C. The temperature in the axis of the charge being heated at the furnace exit is in the range of 1160–1180 °C depending on where the temperature is measured. Considering, in turn, the temperature fluctuations of the exhaust gas (Figure 7b), one can clearly see large temperature oscillations, occasionally reaching 140 °C. Here, too, a large asymmetry in temperature distribution across the width of the furnace can be observed, particularly evident in the preheating and heating zones, where the temperature at points close to the axis of symmetry of the furnace is noticeably higher than that at points closer to the furnace walls (even 160 °C). The balance study was carried out under actual production conditions, at near maximum capacity. Average values recorded by the automation system of the furnace automation were used for the calculations. The basic characteristics of the furnace operation are presented in Table 4. The average natural gas flow rate during the test was 4664 m^3/h. Air was heated in the exhaust gas recuperator to a temperature of 440 °C. The exhaust gas after the furnace chamber had a temperature of 864 °C.

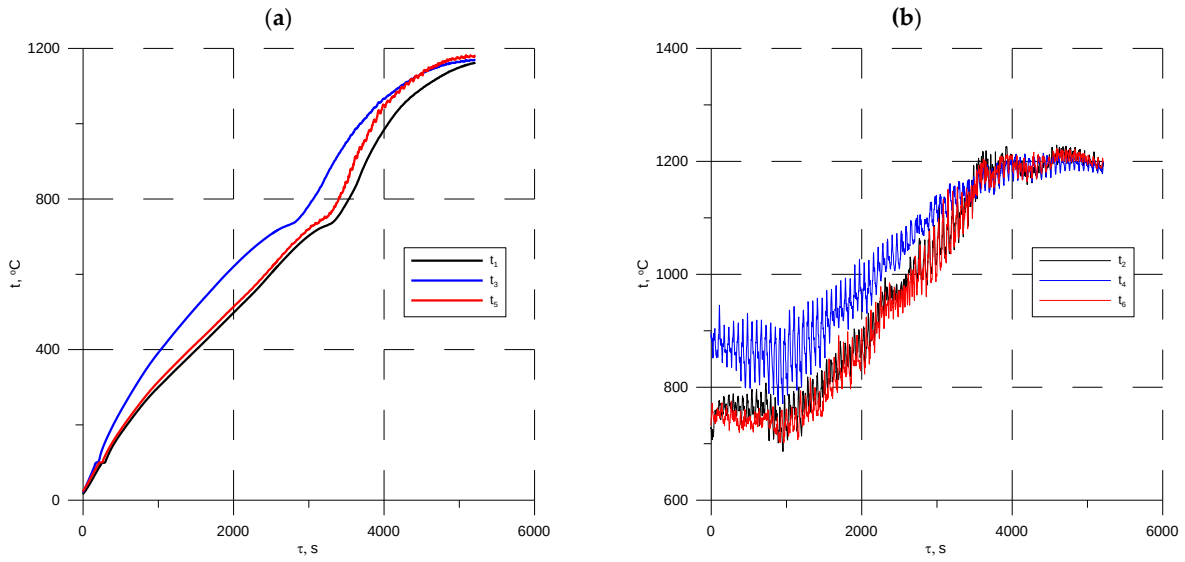

Figure 7. Temperature fluctuations: (**a**) the charge axis, and (**b**) the exhaust gas axis during the heating at selected measurement points; t_1, t_2—left; t_3, t_4—centre; t_5, t_6—right.

Table 4. Data used for the heat balance of the walking-beam furnace.

No.	Name	Value
1.	Gas flow rate	4664 m^3/h
2.	Combustion air	440 °C
3.	Exhaust gas at the outlet of the furnace	864 °C
4.	Composition of dry exhaust gas	$[CO_2]$ = 0.1099 m^3 CO_2/m^3 of dry exhaust gas; $[O_2]$ = 0.0131 m^3 O_2/m^3 of dry exhaust gas; $[N_2]$ = 0.877 m^3 N_2/m^3 of dry exhaust gas;
5.	Cooling water	Mass flow rate 362.5 m^3/h Temperature at the inlet: 28.2 °C Temperature at the outlet: 33.3 °C
6.	Mill scale	0.4% of the mass of the charge
7.	Recuperator	Exhaust gas at the inlet: 830 °C Exhaust gas at the outlet: 735 °C Exhaust gas volumetric flow rate at the inlet: 42,056 m^3/h

Balance calculations were carried out according to the methodology presented in the works of Chen [12] and Ertem [13]. The heat balance equation for the furnace is as follows:

$$\dot{I}_4 + \dot{I}_5 + \Delta\dot{I}_{ch\mathrm{Fe}} = \dot{I}_u + \dot{I}_3 + \dot{I}_6 + \Delta\dot{I}_{ch\text{ł}} + \dot{Q}_{ot} \quad (1)$$

where:

$\dot{I}_3$—enthalpy flow rate of mill scale entered into the furnace, W;

$\dot{I}_4$—enthalpy flow rate of the fuel, W;

$\dot{I}_5$—enthalpy flow rate of the air supplied to the furnace, W;

$\dot{I}_6$—enthalpy flow rate of the exhaust gas exiting the furnace chamber, W;

$\dot{I}_u$—useful enthalpy flow rate of the process (heating of the charge), W;

$\Delta\dot{I}_{ch\text{ł}}$—enthalpy increase of furnace cooling water, W;

$\Delta\dot{I}_{chFe}$– chemical enthalpy flow rate of iron oxidised in the furnace, W;

$\dot{Q}_{ot}$—heat loss to the environment, W.

A natural gas temperature of 0 °C was used to determine the enthalpy flux, hence only the chemical enthalpy was taken into consideration:

$$\dot{I}_4 = \dot{V}_4 Q_i \tag{2}$$

where:

$\dot{V}_4$—gas flow rate, m^3/s;

Q_i—calorific value, J/m^3.

The amount of energy supplied with air, in turn, was defined as follows:

$$\dot{I}_5 = \dot{V}_5 i_5|_{t_0}^{t_5} \tag{3}$$

where:

$\dot{V}_5$—air flow rate, m^3/s;

$i_5|_{t_0}^{t_5}$—enthalpy of air heated from temperature t_0 to t_5, J/m^3.

The chemical enthalpy flux of iron oxidised in the furnace was determined from the enthalpy of devaluation:

$$\Delta\dot{I}_{chFe} = \dot{m}_{Fe}(d_n)_{Fe} \tag{4}$$

where:

$\dot{m}_{Fe}$—mass flow rate of the iron oxidised in the furnace, kg/s;

$(d_n)_{Fe}$—enthalpy of devaluation of the iron, J/kg.

The amount of energy required to heat the charge was calculated as follows:

$$\dot{I}_u = \left(\dot{m}_1 - \dot{m}_{Fe}\right)\ c_{st}|_{t_1}^{t_2}\ (t_2\ - t_1\ ) \tag{5}$$

where:

$\dot{m}_1$—mass flow rate of the charge being heated in the furnace, kg/s;

$c_{st}|_{t_1}^{t_2}$—average specific heat of the charge over the temperature range t_1 to t_1, J/kgK.

The enthalpy of the scale entered into the furnace was calculated taking into account the physical and chemical enthalpy flow rates:

$$\dot{I}_3 = \dot{m}_3\ c_3|_{t_0}^{t_3}\ (t_3\ - t_0\ ) + \dot{m}_3(d_n)_3 \tag{6}$$

where:

$\dot{m}_3$—mass flow rate of the scale entering the furnace, kg/s;

$c_3|_{t_0}^{t_3}$—average specific heat of the scale over the temperature range t_0 to t_3, J/kgK;

$(d_n)_3$—enthalpy of devaluation of the scale, J/kg.

The amount of energy discharged with the exhaust gas is also a loss:

$$\dot{I}_6 = \dot{V}_6\ \ i_6|_{t_0}^{t_6} \tag{7}$$

where:

$\dot{V}_6$—air flow rate, m^3/s;

$i_6|_{t_0}^{t_6}$—enthalpy of the exhaust gas leaving the furnace chamber in the temperature range from t_0 to t_6, J/m^3.

The enthalpy gain of the flow of the water cooling the furnace components was also determined:

$$\Delta\dot{I}_{chł} = \dot{V}_8\ \rho_8\ \ c_8|_{t_8}^{t_9}\ (t_9 - t_8) \tag{8}$$

where:

$\dot{V}_8$—volumetric flow rate of the cooling water, m^3/s;

$c_3|_{t_0}^{t_3}$—average specific heat of the cooling water over the temperature range t_8 to t_9, J/kgK;

The closing figure in the balance is heat loss to the environment:

$$\dot{Q}_{ot} = \dot{I}_4 + \dot{I}_5 + \Delta\dot{I}_{chFe} - \dot{I}_u - \dot{I}_3 - \dot{I}_6 - \Delta\dot{I}_{ch\dot{Z}} \quad (9)$$

Based on the balance calculations, the thermal efficiency of the furnace was determined:

$$\eta_c = \frac{\dot{I}_u}{\dot{I}_4} \quad (10)$$

The value obtained was 69.2%, which corresponds to the conditions of correct furnace operation. This value is comparable with modern designs of continuous furnaces. However, in the case of the recuperator, its efficiency calculated from Equation (2) was 41.2%. This value differs from the leading designs of industrial recuperators [14].

$$h_r = \frac{\dot{I}_5}{\dot{I}_6} \quad (11)$$

The individual items in the balance are presented in a Sankey diagram. Figure 8 shows that more than 20% of the energy is irretrievably lost to the environment with the exhaust gas, which is acceptable considering other designs of industrial furnaces. Based on the heat balance, it can be concluded that changes to the recuperator design are necessary. The firing system of the furnace also requires special attention. During the measurements of the charge temperature, significant temperature fluctuations were found along the length of the charge being heated.

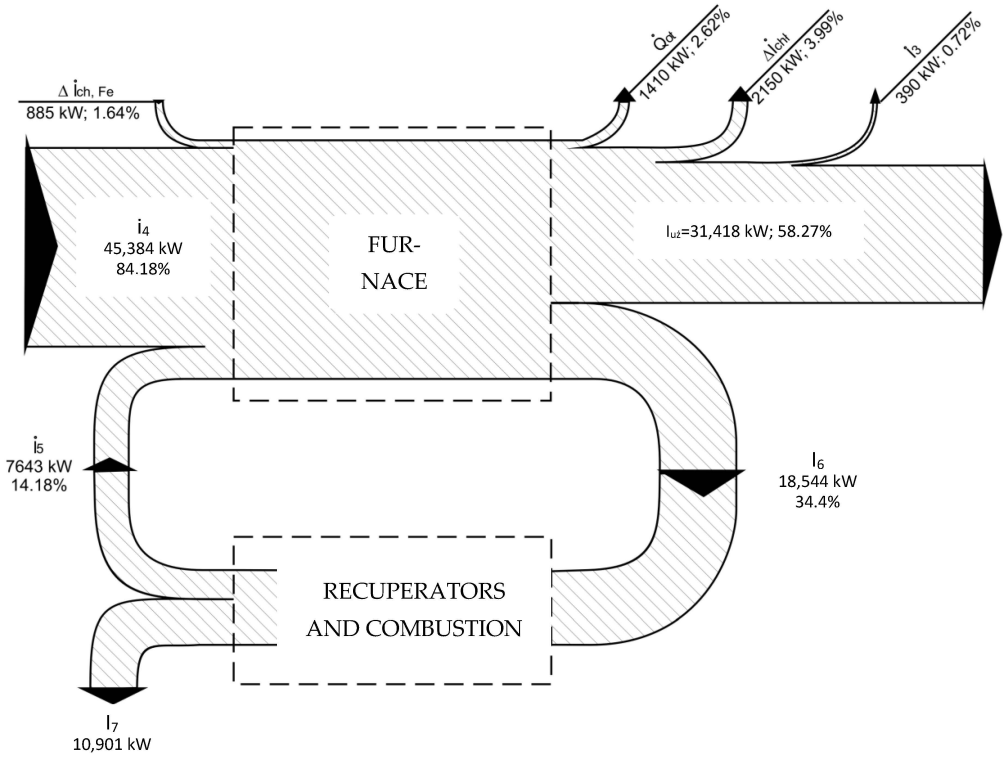

Figure 8. Heat balance of the furnace—Sankey diagram.

3. Numerical Simulation

For the furnace operation variant presented in Section 3, numerical calculations were carried out using thermodynamic process simulation software commonly used in the

power industry, namely IPSEpro 7.0. For the calculations, the built-in balance models representing the individual stages of thermodynamic cycles were used. The energy balance is also the basis for verifying the correctness of the numerical models built. Figure 9 shows a model of the furnace operation. The results of the comparative calculations are presented in Table 5. The composition and volumetric flow rate of the natural gas and the temperature and volumetric flow rate of the combustion air were taken as constant values. The remaining parameters were determined using the model developed. A high agreement was found between the results obtained and the reference values, especially with regard to the composition and temperature of the exhaust gas, as well as the flow rate of the heat from the combustion of natural gas and that of the heat transferred to the charge. As it turned out during the experimental tests, the large difference in the amount of heat transferred in the recuperator to the air being heated was due to the fact that the exhaust gas was diluted with additional air to protect the recuperator.

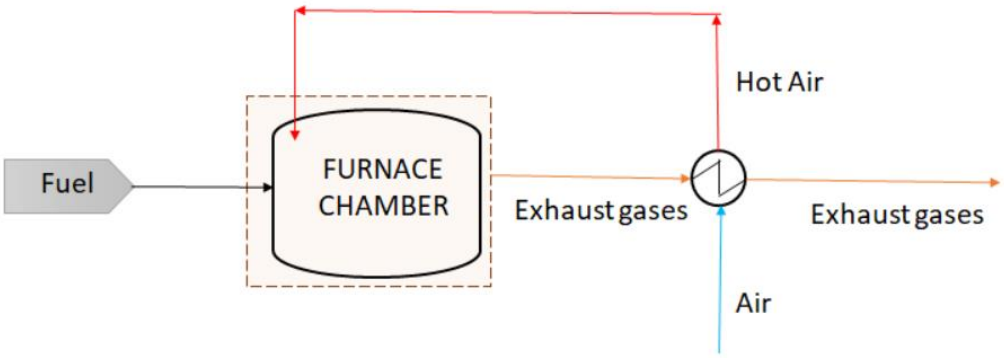

Figure 9. Heating furnace operation model developed in IPSEpro 7.0.

Table 5. Data for heat balance of the walking-beam furnace.

No.	Name	Reference Value	Comparative Calculations
1.	Gas flow rate [m^3/h]	4664	
2.	Combustion air [°C]	440	
3.	Exhaust gas at the outlet of the furnace [°C]	864	844
4.	Composition of dry exhaust gas [m^3/m^3]	$[CO_2]$ = 0.1099 $[O_2]$ = 0.0131 $[N_2]$ = 0.877	$[CO_2]$ = 0.0967 $[O_2]$ = 0.0133 $[N_2]$ = 0.8897
5.	Recuperator	Exhaust gas at the inlet: 830 °C Exhaust gas at the outlet: 735 °C Exhaust gas volumetric flow rate at the inlet: 42,056 m^3/h	Exhaust gas at the inlet: 844 °C Exhaust gas at the outlet: 735 °C Exhaust gas volumetric flow rate at the inlet: 66,046 m^3/h
6.	Heat of gas combustion [kW]	45,384	53,229
7.	Heat transferred to the charge [kW]	31,418	40,037
8.	Heat absorbed in the recuperator [kW]	7643	3256

This fact could not be recorded in the balance calculations due to the balance calculation methodology (balance boundary routed at the actual locations of sampling and measurement of the balance values). The differences in the other values presented, on

the other hand, are largely due to the research methodology adopted. The balancing of heating systems is a stationary process that does not take into account changes in the actual conditions, which requires the averaging of certain values that are subject to large variations in reality, such as temperature, volumetric flow rate, and the quantity of mill scale. Calculations made with IPSEpro reflect the conditions of an ideal stationary process (Figure 9). As a result, there may be some discrepancies in the results obtained. Considering the purpose of the calculations carried out to determine the applicability of hydrogen in metallurgical furnaces, the results obtained with the numerical model should be considered as correct.

In the next step, calculations were carried out to assess the effect of the addition of hydrogen in a mixture with natural gas on the heating conditions of the charge in the walking-beam furnace in three variants, i.e., 100% natural gas; 70% natural gas and 30% hydrogen; 100% hydrogen. For all the calculation tests, the following assumptions were made based on previous reference results (Table 4):

- Fixed quantity of heat transferred to the charge;
- Fixed temperature of the air heated in the recuperator;
- Fixed exhaust gas temperature after the recuperator.

The determined values of the flow rates of the gas and the combustion air allowing for the charge to achieve the temperature assumed in the heating technology are shown in Figure 10. The diagram concerns stoichiometric values.

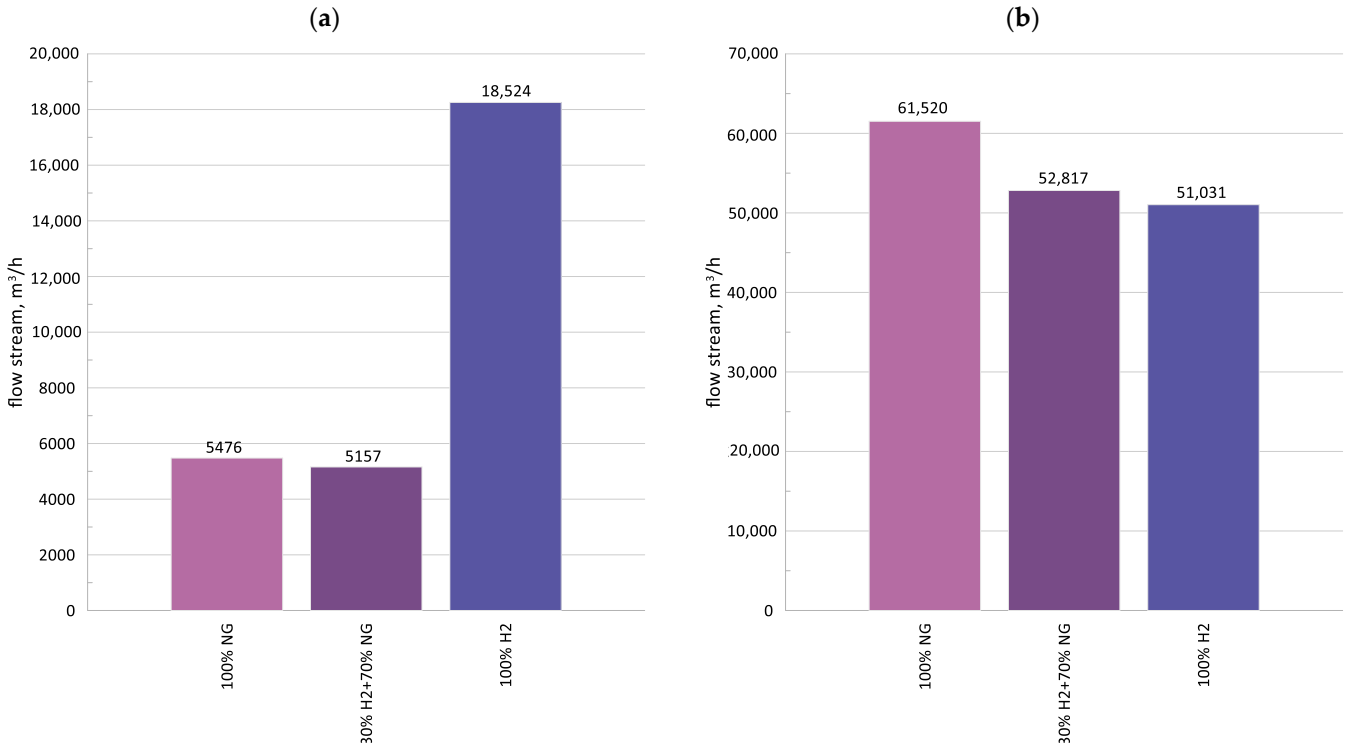

Figure 10. Flow rates of gas (**a**) and combustion air (**b**) for each design variant.

The small addition of hydrogen causes a reduction in the volumetric flow rate of the gas supplied to the combustion chamber. This effect is due to the change in density of the gas mixture due to the addition of hydrogen.

The effect of the excess combustion air ratio on the process parameters was then calculated. Figures 11–13 show the exhaust gas and combustion air flow rates and the exhaust gas temperature at the input and output of the recuperator for three design variants. Figure 11 is a confirmation of the correct operation of the model; the exhaust gas volume is within the range of 64,000 to 94,000 m^3/h. The exhaust gas temperature before the

recuperator, on the other hand, is 904 °C for the stoichiometric ratio of excess combustion air. In industrial tests, this value was much lower due to the high-temperature protection of the recuperator. For a hydrogen content of 30% in the gas mixture (Figure 12), the exhaust gas flow rate ranged from 60,000 to more than 87,000 m^3/h. This means that there will be no need for changes to the exhaust system. Then, the temperature at the inlet to the recuperator was 1035 °C for stoichiometric conditions, higher by more than 100 °C than when burning natural gas. Verification of the exhaust gas cooling system before the recuperator is required regarding the fan capacity. The combustion of pure hydrogen (Figure 13) did not significantly raise the exhaust gas temperature before the recuperator (950 °C under stoichiometric conditions). The heat was absorbed during the heating of the charge. However, the temperature of the exhaust gas before the recuperator increases with increasing quantity of combustion air, compared with the other design variants, amounting to 812 °C for 50% excess combustion air.

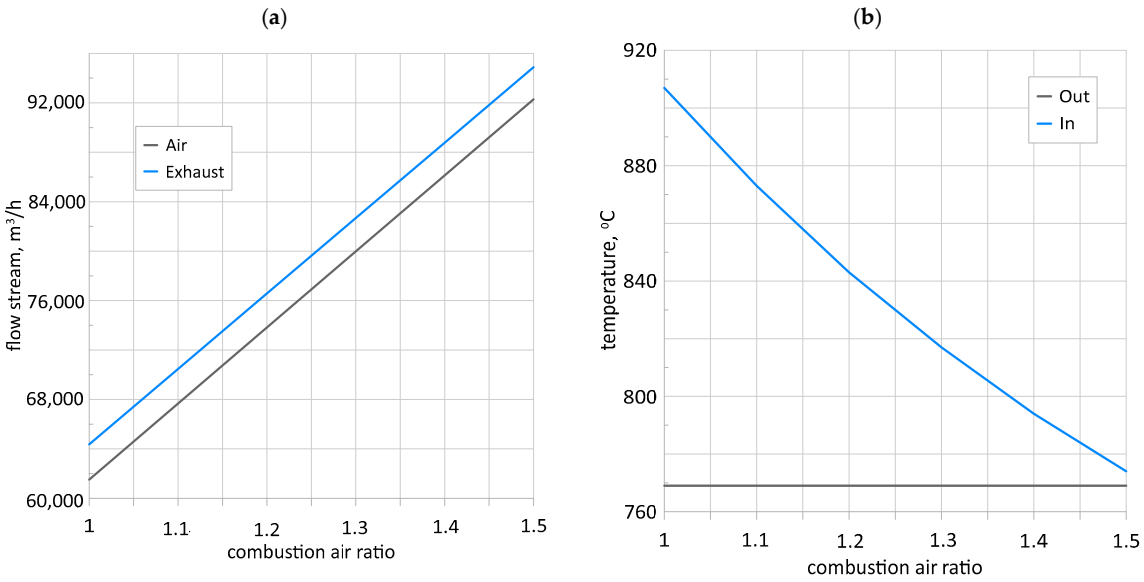

Figure 11. Flow rates of exhaust gas and combustion air (**a**) and exhaust gas temperature upstream and downstream of the recuperator (**b**)—100% natural gas.

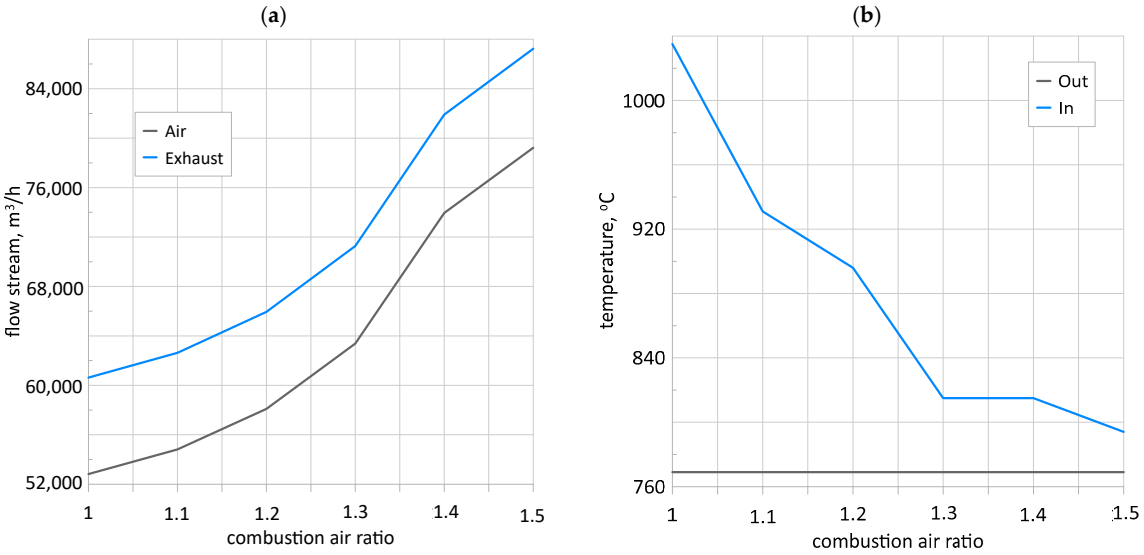

Figure 12. Flow rates of exhaust gas and combustion air (**a**) and exhaust gas temperature upstream and downstream of the recuperator (**b**)—30% H_2.

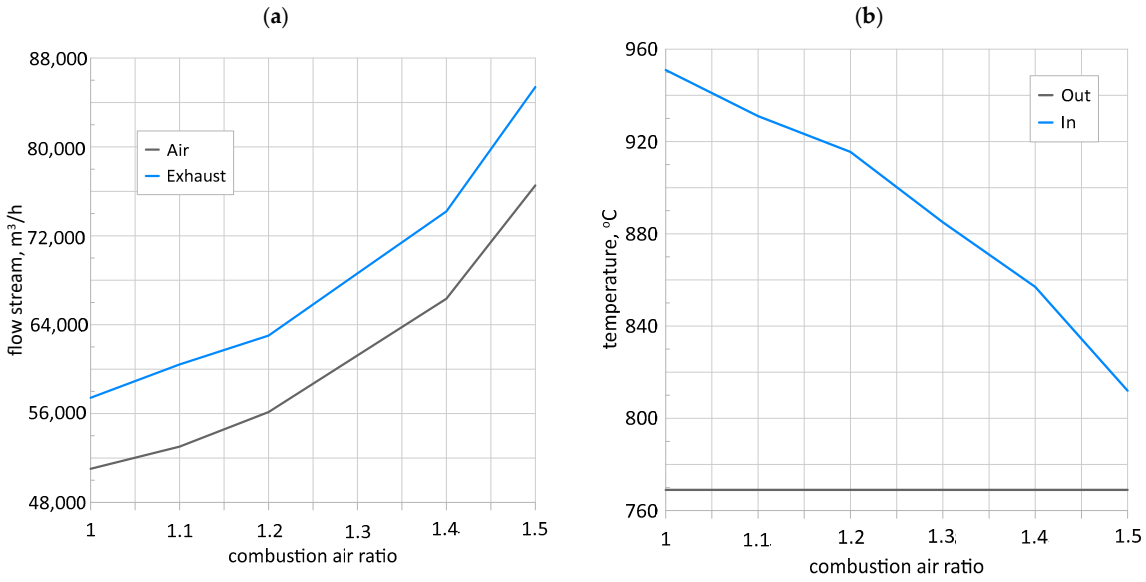

Figure 13. Flow rates of exhaust gas and combustion air (**a**) and exhaust gas temperature upstream and downstream of the recuperator (**b**)—100% hydrogen.

4. Summary and Conclusions

4.1. Heat Balance of the Furnace

This paper presents a technical analysis of the feasibility of using hydrogen to fire furnaces used in the metallurgical sector. For this purpose, tests were carried out on a walking-beam furnace to determine its thermal indices. The particular characteristic of the furnace under consideration indicates that approx. 45.4 MW of energy contained in fuel must be supplied at the rated output of the furnace. Balance studies have shown that approx. 70% of the fuel energy is usefully utilised in the charge heating process (at a furnace thermal efficiency of 69.2%). In counter-flow furnaces, this value ranges from approx. 60% for low-efficiency furnaces, to 80% for high-efficiency furnaces. The furnace under consideration is thus a medium-efficient device with regard to the energy performance characteristic examined. Approx. 41% of the fuel energy is discharged from the furnace with the exhaust gas. This is a large proportion of the fuel energy. Although about 40% of the energy output from the furnace is recovered by the recuperation system, up to 24% of the fuel energy is discharged with the exhaust gas to the environment. This adverse effect in terms of energy efficiency is mainly due to the excessively high temperature of the exhaust gas leaving the furnace chamber and the necessary (protective) cooling of the exhaust gas for the recuperator. The current recuperation system is a poor solution. The recuperator was designed either for a longer furnace or for the existing furnace at a lower capacity, while the exhaust gas cooling was designed at a later time for the conditions under which the furnace in question is overloaded. The consequence of the current design of the recuperation system is low recuperation efficiency. Under the conditions of the test carried out, the recuperation efficiency was low at around 41%. If the exhaust gas discharged from the furnace had a temperature equal to that of air-cooled exhaust gas, the recuperation efficiency would be approx. 47%. Considering the recuperation efficiency, this is a clear increase.

The heat balance showed that the energy transferred from the furnace by the cooling water is 4.7% of the chemical energy of the fuel. For counter-flow furnaces, this value is in the range of 2 to 3%. It can therefore be seen that these losses can be reduced; however, it is difficult to expect a significant change in the energy efficiency of the furnace by upgrading the cooling system. Nevertheless, the possibility of upgrading the cooling system can be considered through a techno-economic analysis.

The heat balance also showed that the heat lost by the furnace to the environment was about 3.1%. For counter-flow furnaces, this value is in the range of 1 to 3%. It can therefore be concluded that this balance item is correct. However, it should be noted

that the flow rate of heat discharged to the environment was calculated from the balance equation, which means that the calculated value may be slightly higher, as it includes all the balance errors. The heat loss to the environment can only be reduced by retrofitting the lining that thermally insulates the furnace. In equipment that is often switched off, the insulating lining uses fibrous materials placed on the inside of the furnace refractory. This is an effective way of reducing energy losses associated with heat accumulation and cutting down heat loss through the refractory. Unfortunately, fibrous materials have an unfavourable emission factor, which means that the efficiency of radiation heat transfer deteriorates. The techno-economic analysis must therefore take into account the impact of this process on the heating technology. This is an issue of particular relevance to the furnace under consideration because the temperature of the exhaust gas at the outlet of the furnace chamber was already too high at the performance level during the tests.

4.2. Hydrogen in Furnaces

A numerical model was then developed using the IPSEpro software to determine the amount of gas, the resulting exhaust gas, and the impact on the thermal parameters of the heating system. The calculations were made for pure natural gas, 30% hydrogen content, and hydrogen alone. It was found that no changes would be required to the exhaust gas discharge system, while the fan supplying air for exhaust gas cooling before the recuperator would need to be redesigned. The amount of hydrogen required to fire the walking beam furnace increases significantly (by a factor of almost 3), which may have an impact on the operating costs. On the other hand, carbon dioxide emissions into the atmosphere are completely reduced, which may be crucial when considering possible options for upgrading furnace units operating in the metallurgical industry in an era of climate warming.

Author Contributions: Conceptualization, K.S. and A.G.; methodology, A.G.; formal analysis K.S. and A.G.; investigation, K.S. and A.G.; data curation, A.G.; writing—original draft preparation, K.S. and A.G.; writing—review and editing, K.S. and A.G.; visualization, K.S. and A.G.; supervision, Ł.M. and K.S.; project administration, Ł.M. and A.G.; funding acquisition, Ł.M. and A.G. All authors have read and agreed to the published version of the manuscript.

Funding: This research was funded by the Ministry of Science and Higher Education, Poland, AGH grant No. 16.16.210.476, and partly supported by the Excellence Initiative—Research University programme of the AGH University of Krakow.

Data Availability Statement: The data presented in this study are available on request from the corresponding author.

Conflicts of Interest: The authors declare no conflicts of interest.

References

1. EU Council and European Council Energy Prices and Security of Supply. Available online: https://www.consilium.europa.eu/pl/policies/energy-prices-and-security-of-supply/#EU (accessed on 1 June 2024).
2. Eurostat Electricity and Heat Statistics. Available online: http://ec.europa.eu/eurostat/statistics-explained/index.php/Electricity_and_heat_statistics (accessed on 1 June 2024).
3. Erbach, G.; Jensen, L. EU Hydrogen Policy Hydrogen as an Energy Carrier for a Climate-Neutral Economy. 2021. Available online: https://www.europarl.europa.eu/thinktank/en/document/EPRS_BRI(2021)689332 (accessed on 1 May 2024).
4. Adolf, J.; Balzer, C.H.; Louis, J.; Schabla, U.; Fischedick, M.; Arnold, K.; Pastowski, A.; Schüwer, D. *Sustainable Mobility through Fuel Cells and H_2*; Shell Deutschland Oil: Hamburg, Germany, 2017; 37p.
5. SSAB HYBRIT®. A New Revolutionary Steelmaking Technology. Available online: https://www.ssab.com/en/fossil-free-steel/insights/hybrit-a-new-revolutionary-steelmaking-technology (accessed on 1 May 2024).
6. IEA Iron and Steel Technology Roadmap. 2020. Available online: https://www.oecd-ilibrary.org/energy/iron-and-steel-technology-roadmap_3dcc2a1b-en (accessed on 1 May 2024).
7. Dise Energy and PWEA. Green Hydrogen from RES in Poland of the EU Climate and Energy Policy in Poland. 2021. Available online: https://www.psew.pl/en/ (accessed on 1 May 2024).
8. Muron, M.; Pawelec, G.; Jackson, S.; Yovchev, I.-P. Clean Hydrogen Monitor. 2022, pp. 30–80. Available online: https://www.h2knowledgecentre.com/content/policypaper2174 (accessed on 1 May 2024).

9. Williams, A.F. *Combustion Theory*, 2nd ed.; CRC Press: Boca Raton, FL, USA, 1985; ISBN 9780429494055.
10. Jerzak, W. Adiabatic flame temperature and laminar burning velocity of CH4/H2/air mixtures (in Polish). *Arch. Spalania* **2012**, *11*, 197–206.
11. Fluke Process Instruments. *Furnace Tracker System. User Manual*; Fluke Process Instruments: Cambridge, UK, 2004.
12. Chen, W.H.; Chung, Y.C.; Liu, J.L. Analysis on energy consumption and performance of reheating furnaces in a hot strip mill. *Int. Commun. Heat Mass Transf.* **2005**, *32*, 695–706. [CrossRef]
13. Ertem, M.E.; Şen, S.; Akar, G.; Pamukcu, C.; Gurgen, S. Energy balance analysis and energy saving opportunities for erdemir slab furnace #3. *Energy Sources Part A Recover. Util. Environ. Eff.* **2010**, *32*, 979–994. [CrossRef]
14. Trinks, W.; Mawhinney, M.H.; Shannon, R.A.; Reed, R.J.; Garvey, J.R. *Industrial Furnaces*; John Wiley & Sons, Inc.: Hoboken, NJ, USA, 2004; ISBN 9780471387060.